TUM-HEP-494/02

Capabilities of Future Long Baseline Neutrino Oscillation Experiments*

M. Lindner

November 27, 2002

Future long baseline neutrino oscillation (LBL) setups are discussed and the remarkable potential for very precise measurements of mass splittings, mixing angles, MSW effects, the sign of Δm^2 and leptonic CP violation is shown.

1 Introduction

The evidence for atmospheric neutrino oscillations shows some sensitivity to the characteristic L/E dependence of oscillations[1]. There is no doubt that the observed flavour transitions are due to neutrino oscillations. The atmospheric oscillation length scale L_{atm} is for $\Delta m^2_{31} \simeq 3 \cdot 10^{-3}$ eV, and for neutrino energies of $E_\nu \simeq 10$ GeV, about $L_{atm} \simeq O(2000)$ km. This are distances and energies which can also be tested with neutrino beams which are sent from one point on the Earth to another. Solar neutrinos also undergo flavour transitions[2, 3]. Oscillation is under all alternatives the most plausible explanation and global fits favour the so-called LMA solution for the mass splittings and mixings[4]. The CHOOZ reactor experiment[5] provides moreover currently the most stringent upper bound for the sub-leading U_{e3} mixing matrix element. The global pattern of neutrino oscillation parameters seems therefore quite well known and one may ask how precise future experiments will ultimately be able to measure mass splittings and mixings and what can be learned from such precise measurements.

K2K, MINOS and CNGS are a promising first generation of LBL experiments. We discuss[6] here the remarkable potential beyond this first generation, where detailed tests of the three-flavouredness of oscillations will be possible. θ_{13} can be measured much better than today. It will be possible to study MSW matter effects and to extract $sign(\Delta m^2_{31})$.

*To appear in the proccedings of the IDM2002 conference, Sept. 2-6, 2002, York, UK

For the favoured LMA case, it will even be possible to measure leptonic CP violation[7]. Such precise neutrino masses, mixings and CP phases constitutes extremely valuable flavour information, since unlike for quarks, they are not obscured by hadronic uncertainties. These parameters can be evolved with the renormalization group to the GUT scale to be compared with models for neutrino masses and mixings. Leptonic CP violation is moreover related to leptogenesis, the currently most plausible mechanism for the generation of the baryon asymmetry of the universe. LBL experiments offer therefore in a unique way access to extremely interesting and valuable physics parameters.

2 Beams and Detectors

LBL experiments have the advantage that both source and detector can be kept under precise conditions. This includes amongst others for the source a precise knowledge of the mean neutrino energy E_ν, the neutrino flux and spectrum, as well as the flavour composition and contamination of the beam. Another important aspect is whether neutrino and anti-neutrino data can be obtained symmetrically such that systematical uncertainties cancel. Precise measurements require also a sufficient luminosity and a detector such that enough statistics can be obtained. On the detector side one must include further issues, like the detection threshold function, energy calibration, resolution, particle identification capabilities (flavour, charge, event reconstruction, backgrounds). Another source of uncertainty in the detection process is the knowledge of neutrino cross-sections, especially at low energies[8]. Source and detector combinations of a future LBL experiment are furthermore constraint by the available technology.

The first type of considered sources are conventional neutrino and anti-neutrino beams. An intense proton beam is typically directed onto a massive target producing mostly pions and some K mesons, which are captured by an optical system of magnets in order to obtain a beam. The pions (and K mesons) decay in a decay pipe, yielding essentially a muon neutrino beam which can undergo oscillations as shown in the left plot of fig. 1. Most interesting are the $\nu_\mu \to \nu_\mu$ disappearance channel and the $\nu_\mu \to \nu_e$ appearance channels. The neutrino beam is, however, contaminated by approximately 0.5% electron neutrinos, which also produce electron reactions in the disappearance channel, limiting thus the precision in the extraction of $\nu_\mu \to \nu_e$ oscillation parameters. The energy spectrum of the muon beam can be controlled over a wide range: it depends on the incident proton energy, the optical system, and the precise direction of the beam axis compared to the direction of the detector. It is possible to produce broad band high energy beams, such as the CNGS beam[9, 10], or narrow band lower energy beams, such as in some configurations of the NuMI beam[11]. Reversing the electrical current in the lens system results in an anti-neutrino beam. The neutrino and anti-neutrino beams have significant differences such that errors do not cancel systematically in ratios or differences. The neutrino and anti-neutrino beams must therefore

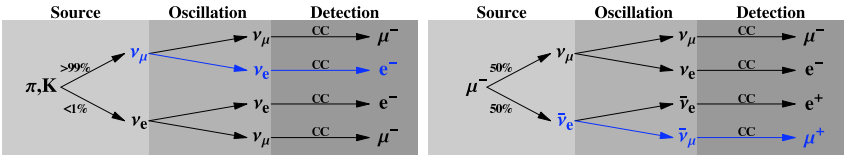

Figure 1: Neutrino production, oscillation and detection via charged current interactions for conventional beams (left plot) and superbeams (right plot). The $\nu_\mu \to \nu_\mu$ disappearance and $\nu_\mu \to \nu_e$ appearance channels are most interesting for the conventional beams, but the ν_e beam contamination at the level of $< 1\%$ limits the ability to determine the $\nu_\mu \to \nu_e$ appearance oscillation, since it produces also electrons. For neutrino factories (right plot) $\bar{\nu}_e$ and ν_μ are produced in equal numbers from μ-decays and can undergo different oscillations. The $\nu_\mu \to \nu_\mu$ and $\bar{\nu}_e \to \bar{\nu}_\mu$ channels are most interesting for detectors with μ identification. Note, however, that excellent charge identification capabilities are required to separate "wrong sign muons" and "right sign muons".

more or less be considered as independent sources with different systematical errors.

"Superbeams" use the same techniques for producing neutrino beams, but at much larger luminosities [9, 10, 11, 12]. Superbeams are thus a technological extrapolation of conventional beams, with a proton beam intensity close to the mechanical stability limit of the target at a typical thermal power of 0.7 MW to 4 MW. The much higher neutrino luminosity allows the use of the decay kinematics of pions to produce so–called "off–axis beams", where the detector is located some degrees off the beam axis. This reduces the neutrino flux and the average neutrino energy, but leads to a more mono-energetic beam and a significant suppression of the electron neutrino contamination. Several off–axis superbeams with energies of about 1 GeV to 2 GeV have been proposed in Japan[13, 14], America[15], and Europe[16, 17].

The most sensitive neutrino oscillation channel for sub-leading oscillation parameters is the $\nu_\mu \to \nu_e$ appearance transition. Therefore the detector should have excellent electron and muon charged current identification capabilities. In addition, an efficient rejection of neutral current events is required, because the neutral current interaction mode is flavor blind. With low statistics, the magnitude of the contamination itself limits the sensitivity to the $\nu_\mu \to \nu_e$ transition severely, while the insufficient knowledge of its magnitude constrains the sensitivity for high statistics. A near detector allows a substantial reduction of the background uncertainties[13, 18] and plays a crucial role in controlling other systematical errors, such as the flux normalization, the spectral shape of the beam, and the neutrino cross section at low energies. At energies of about 1 GeV, the dominant charge current interaction mode is quasi–elastic scattering, which suggests that water Cherenkov detectors are the optimal type of detector. At these energies, a baseline of about 300 km would be optimal to measure at the first maximum of the oscillation. At about 2 GeV, there is already a considerable contribution of inelastic scattering to the charged current interactions, which

means that it would be useful to measure the energy of the hadronic part of the cross section. This favors low–Z hadron calorimeters, which also have a factor of ten better neutral current rejection capability compared to water Cherenkov detectors[15]. In this case, the optimum baseline is around 600 km. The matter effects are expected to be small for these experiments for two reasons. First of all, an energy of about 1 GeV to 2 GeV is small compared to the MSW resonance energy of approximately 13 GeV in the upper mantle of the Earth. The second reason is that the baseline is too short to produce significant matter effects.

The second type of beam considered are so-called neutrino factories, where muons are stored in the long straight sections of a storage ring. The decaying muons produce muon and electron anti-neutrinos in equal numbers[19]. The muons are produced by pion decays, where the pions are produced by the same technique as for superbeams. After being collected, they have to be cooled and reaccelerated very quickly. The spectrum and flavor content of the beam are completely characterized by the muon decay and are therefore very precisely known[20]. The only adjustable parameter is the muon energy E_μ, which is usually considered in the range from 20 to 50 GeV. It is possible to produce and store anti-muons in order to obtain a CP conjugated beam and the symmetric operation of both beams leads to the cancellation or significant reduction of errors and systematical uncertainties. Unless stated differently, we discuss the neutrino beam including implicitly the CP conjugate channel.

The decay of the muons and the relevant oscillation channels are shown in the right plot of fig. 1. Amongst all flavors and interaction types, muon charged current events are the easiest to detect. The appearance channel with the best sensitivity is thus the $\bar{\nu}_e \to \bar{\nu}_\mu$ transition, which produces so called "wrong sign muons". Therefore, a detector must be able to very reliably identify the charge of a muon in order to distinguish wrong sign muons in the appearance channel from the higher rate of same sign muons in the disappearance channels. The dominant charge current interaction in the multi–GeV range is deep–inelastic scattering, making a good energy resolution for the hadronic energy deposition necessary. Magnetized iron calorimeters are thus the favored choice for neutrino factory detectors. In order to achieve the required muon charge separation, it is necessary to impose a minimum muon energy cut at approximately[21, 22] 4 GeV. This leads to a significant loss of neutrino events in the range of about 4 GeV to 20 GeV, which means that a high muon energy of $E_\mu = 50$ GeV is desirable. The first oscillation maximum lies then at approximately 3 000 km. Matter effects are sizable at this baseline and energy, and the limited knowledge of the Earth's matter density profile becomes an additional source of errors.

acronym	detector	L	L/E_{peak}
JHF-SK	water Cherenkov	295	378
NuMI	low-Z	735	337
NuFact-I	10 kt mag. iron	3000	90
JHF-HK	water Cherenkov	735	295
NuFact-II	40 kt mag. iron	3000	90

Table 1: The considered combinations of beams and detectors and their acronyms.

3 Results of LBL Simulations

The physics which enters the above setups can be understood analytically by expanding in small quantities[23, 24, 25]. All shown results can thus be understood qualitatively with analytic equations[6], but they are obtained in a numerical simulation of the exact oscillation equations. There are numerous experimental and phenomenological details which have to be included in such analysis which go beyond the scope of this article[6].

We consider different beams and detectors which allow interesting combinations as listed in table 1. JHF-SK is the planned combination of the existing SuperKamiokande detector and the JHF beam, while JHF-HK is the combination of an upgraded JHF beam with the proposed HyperKamiokande detector. With typical parameters, JHF-HK is altogether about 95 times more integrated luminosity than JHF-SK, and we assume that it operates partly with the anti-neutrino beam. Water Cherenkov detectors are ideal for the JHF beam, since charged current quasi elastic scattering is dominating. A low-Z calorimeter is proposed for the NuMI off-axis beam, which is better here, since the energy is higher and there is already a considerable contribution of inelastic charged current interactions. NuFact-I is an initial neutrino factory, while NuFact-II is a fully developed machine, with 42 times the luminosity of NuFact-I[13, 15, 21]. Deep inelastic scattering dominates for these even higher energies and magnetized iron detectors are therefore considered in combination with neutrino factories.

Our study includes all relevant aspects[6] and we find the following results. There is excellent precision for the leading oscillation parameters Δm^2_{31} and $\sin^2 2\theta_{23}$, which will not be further discussed here. The more interesting sensitivity to the sub-leading parameter $\sin^2 2\theta_{13}$ depends on what will be found for Δm^2_{31} and Δm^2_{21}. Assuming that the leading parameters are measured to be $\Delta m^2_{31} = 3 \cdot 10^{-3}$ eV^2, $\sin^2 2\theta_{23} = 0.8$ and that KamLand measures the solar parameters at the current best fit point of the LMA region, *i.e.* $\Delta m^2_{21} = 6 \cdot 10^{-5}$ eV^2 and $\sin 2\theta_{12} = 0.91$, we can make a comparison of the $\sin^2 2\theta_{13}$ sensitivity limit for the different setups. The result is shown in the left plot of fig. 2. The individual contributions of different sources of uncertainties are shown for every experiment and the left edge of every band of fig. 2 corresponds to the sensitivity limit which would

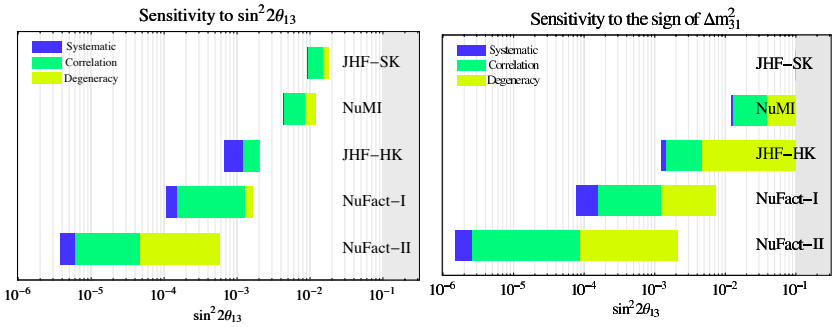

Figure 2: The $\sin^2 2\theta_{13}$ sensitivity (left plot) and the $\sin^2 2\theta_{13}$ sensitivity region to $sign(\Delta m^2_{31})$ (right plot) for all setups defined in section 3 at 90% CL for $\Delta m^2_{31} = 3{\cdot}10^{-3}\,\mathrm{eV}^2$ and $\sin^2 2\theta_{23} = 0.8$. The plots show the deterioration of the sensitivity limits as the different error sources are successively switched on. The left edge of the bars is the sensitivity statistical limit. This limit gets reduced as systematical, correlational and degeneracy errors are switched on. The right edge is the final sensitivity limit [6].

be obtained purely on statistical grounds. This limit is successively reduced by adding the systematical uncertainties of each experiment, the correlational errors and finally the degeneracy errors. The right edge of each band constitutes the final error for the experiment under consideration. It is interesting to see how the errors of the different setups are composed. There are different sensitivity reductions due to systematical errors, correlations and degeneracies. The largest sensitivity loss due to correlations and degeneracies occurs for NuFact-II.

Another challenge of future LBL experiments is to measure $sign(\Delta m^2_{31})$ via matter effects and the sensitivity which can be obtained for the setups under discussion is shown in the right plot of fig. 2. Taking all correlational and degeneracy errors into account we can see that it is very hard to determine $sign(\Delta m^2_{31})$ with the considered superbeam setups. The main problem is the degeneracy with δ, which allows always the reversed $sign(\Delta m^2_{31})$ for another CP phase. Note, however, that the situation can in principle be improved if different superbeam experiments were combined such that this degeneracy error could be removed. Neutrino factories perform considerably better on $sign(\Delta m^2_{31})$, particularly for larger baselines. Combination strategies would again lead to further improvements.

Coherent forward scattering of neutrinos and the corresponding MSW matter effects are so far experimentally untested. It is therefore very important to realize that matter effects will not only be useful to extract $sign(\Delta m^2_{31})$, but that they allow also detailed tests of coherent forward scattering of neutrinos. This has been studied in detail[25, 26, 27, 28].

The Holy Grail of LBL experiments is the measurement of leptonic CP violation. The $\sin^2 2\theta_{13}$ sensitivity range for measurable CP violation is shown in fig. 3 for $\delta = \pi/2$ for the different setups and for different values of Δm^2_{21}. It can be seen that measurements

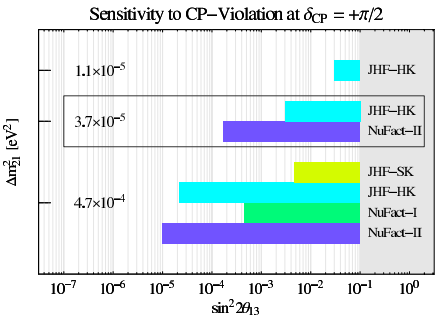

Figure 3: The $\sin^2 2\theta_{13}$ sensitivity range for CP violation of the considered setups at 90% confidence level and for different Δm^2_{21} values. The upper row corresponds to the lower bound of $\Delta m^2_{21} = 1.1 \times 10^{-5}$ eV^2, the bottom row to the upper bound $\Delta m^2_{21} = 4.7 \times 10^{-4}$ eV^2, and the middle row to the best LMA fit, $\Delta m^2_{21} = 3.7 \times 10^{-5}$ eV^2. Cases which do not have CP sensitivity are omitted from this plot. The chosen parameters are $\delta = +\pi/2$, $\Delta m^2_{31} = 3 \cdot 10^{-3}$ eV^2, $\sin^2 2\theta_{23} = 0.8$, and a solar mixing angle corresponding to the current best fit in the LMA regime [6].

of CP violation are in principle feasible both with high luminosity superbeams as well as advanced neutrino factories. However, the sensitivity depends in a crucial way on Δm^2_{21}. For a low value $\Delta m^2_{21} = 1.1\ 10^{-5}$ eV^2, the sensitivity is almost completely lost, while the situation would be very promising for the largest considered value $\Delta m^2_{21} = 4.7\ 10^{-4}$ eV^2. For a measurement of leptonic CP violation it would therefore be extremely exciting and promising if KamLand would find Δm^2_{21} on the high side of the LMA solution (the so-called HLMA case). The sensitivities shown in fig. 3 depend on the choice for δ. The value which was used here was $\delta = \pi/2$ and and the sensitivities become become worse for small CP phases close to zero or π.

4 Conclusions

In Future long baseline neutrino oscillation experiments will lead to precision neutrino physics.

References

[1] T. Toshito (SuperKamiokande Collab.), `hep-ex/0105023`.

[2] Q. R. Ahmad *et al.* (SNO Collab.), Phys. Rev. Lett. **89**, 011301 (2002).

[3] Q. R. Ahmad *et al.* (SNO Collab.), Phys. Rev. Lett. **89**, 011302 (2002).

[4] See e.g. P. C. de Holanda and A. Yu. Smirnov, hep-ph/0205241.

[5] M. Apollonio *et al.* (Chooz Collab.), Phys. Lett. **B466**, 415 (1999).

[6] P. Huber, M. Lindner and W. Winter, hep-ph/0204352.

[7] K. Dick, M. Freund, M. Lindner, A. Romanino, Nucl. Phys. B **562** (1999) 29.

[8] E.A. Paschos, hep-ph/0204138.

[9] G. Acquistapace *et al.* (CNGS Collab.) CERN-98-02.

[10] R. Baldy *et al.* (CNGS Collab.) CERN-SL-99-034-DI.

[11] J. Hylen *et al.* (NuMI Collab.) FERMILAB-TM-2018.

[12] K. Nakamura (K2K Collab.), Nucl. Phys. **A663**, 795 (2000).

[13] Y. Itow *et al.*, hep-ex/0106019.

[14] M. Aoki, hep-ph/0204008.

[15] A. Para and M. Szleper, hep-ex/0110032.

[16] See e.g. J.J. Gomez-Cadenas *et al.*, hep-ph/0105297.

[17] F.Dydak, Rep., CERN (2002), http://home.cern.ch/dydak/oscexp.ps.

[18] M. Szleper and A. Para, hep-ex/0110001.

[19] S. Geer, Phys. Rev. **D57**, 6989 (1998).

[20] Particle Data Group, D.E. Groom *et al.*, Eur.Phys.J. C **15**, 1 (2000).

[21] A. Blondel *et al.*, Nucl. Instrum. Meth. **A451**, 102 (2000).

[22] C. Albright *et al.*, hep-ex/0008064, and references therein.

[23] A. Cervera *et al.*, Nucl. Phys. **B579**, 17 (2000).

[24] M. Freund, Phys. Rev. **D64**, 053003 (2001).

[25] M. Freund, P. Huber, and M. Lindner, Nucl. Phys. **B615**, 331 (2001).

[26] M. Freund, M. Lindner, S. T. Petcov and A. Romanino, Nucl. Phys. **B578**, 27 (2000).

[27] M. Freund, P. Huber, and M. Lindner, Nucl. Phys. **B585**, 105 (2000).

[28] M. Freund, M. Lindner, S.T. Petcov and A. Romanino, Nucl. Instrum. Meth. A **451**, 18 (2000).